



Experimental behavior based on effective slab width acting as a flange with supporting steel beams in composite floors with openings

Magdy Khalaf, Ashraf El-Shihy

Structural Engineering Dept., Faculty of Engineering, Zagazig University, Zagazig, Egypt.
drmagdykhalaf@gmail.com, https://orcid.org/0000-0001-5944-4288
amshihy@yahoo.com

El-Sayed El-Kasaby, Ahmad Youssef

Civil Engineering Dept., Faculty of Engineering, Benha University, Benha, Egypt.
profkasaby@gmail.com, aykmar@yahoo.com

ABSTRACT. An experimental study with many variables was carried out to investigate the effective width of simply supported composite beams (T and L sec. beams) with and without slab opening. Three full-scale composite slab models with six different carrier simply supported composite beams (three with T-sec. and three with L-sec.) with constant slab rectangularity were tested. Each model was loaded by a uniform distributed load (within elastic behavior zone) then loaded by means of two-concentrated loads system acting at equal distances from supports till failure. One of them without slab opening and the others with two symmetric slab openings and constant opening position in direction parallel to main supporting beams longitudinal axes.

In this research, the tested model features, materials properties and measurement instrumentations are described in brief. The maximum load carrying capacity; crack patterns, deflections at different positions and generated strains in form of estimated effective width were experimentally investigated. Interesting gained results were recorded such that more than 100% of slab effective width is preserved for interior supporting beams if the openings are away enough from carried composite slabs structural carried zones while only 70% was preserved for exterior ones. Also, concentrated loads manner reduced carried composite slab effective width to be 85% in average of that recorded for equivalent distributed loads. Some conclusions and recommendations are introduced.

KEYWORDS. Composite; Floors; Experimental; Effective width; Corrugated; Steel; Sheets; Openings.



Citation: Khalaf, M., El-shihy, A., El-Kasaby, E., Youssef, A., Experimental behavior based on effective slab width acting as a flange with supporting steel beams in composite floors with openings, *Frattura ed Integrità Strutturale*, 61 (2022) 308-326.

Received: 11.11.2021
Accepted: 30.05.2022
Online first: 05.06.2022
Published: 01.07.2022

Copyright: © 2022 This is an open access article under the terms of the CC-BY 4.0, which permits unrestricted use, distribution, and reproduction in any medium, provided the original author and source are credited.

INTRODUCTION

Today formed steel deck is very commonly used for composite floor systems. A composite floor type shown in Fig. 1 (which is one of the various types as shown in Figs. 2,3 and 4) will be investigated through the current research to experimentally estimate the effective composite floor width acting as a flange to carrier steel beams.

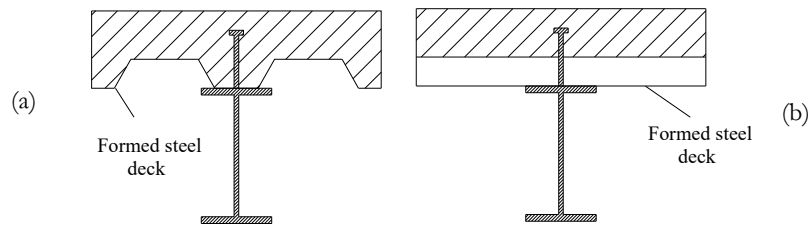


Figure 1: Composite slab with ribbed "corrugated" steel deck. (a) "Beams" ribs parallel (b): "Girders" ribs perpendicular

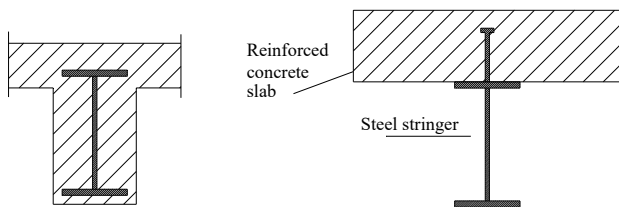


Figure 2: Encased section.

Figure 3: Overlaid section.

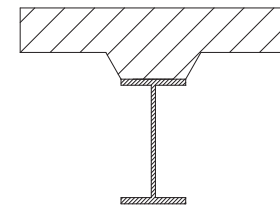


Figure 4: Overlaid section with Haunch.

Some researches [1-4] investigated the problem analytically to estimate width of slab that acts as a part of the beam effectively. If the beams are rather closely spaced, the bending stresses in the slab will be fairly uniformly distributed across compression zone. Otherwise, if in between beams distances are large enough, bending stresses will vary quite a bit and non-linearly across the flange.

The matter of effective width of slab as a flange of beam was investigated firstly by Bortsch [5] and others within elastic range of simply supported beams and later up to now by many others for various loading and boundary conditions. Although early interesting was concerned with traditional reinforced concrete structures (structures of hulls of ships and sheet-stiffeners combinations for aerospace structures with essentially elastic behavior) recent interest has been directed to finding the effective width at ultimate loads depending on deflection calculations from the "limit state of stress" point of view. The effective width used in design is defined as that width of slab that, when acted on by the actual maximum stress, would have the same static equilibrium effect as the existing variable stress. In other words, the effective width is obtained by integrating the longitudinal strain in the slab at the top and dividing by the peak value of strain. Chapman and Teraskiewicz [6] showed that due to the complexity of the problem and the actual behavior of various types of composite beams with monolithic beam-slab construction under complex loading and environmental conditions, simplified formulas for effective width are needed. Other researches numerically extended studies in this subject numerically spotting light on plastic analysis; [7, 8]. Many other researchers; [9-13]; experimentally investigated the problem of effective width for composite slabs without openings. Recently, others re-studied the problem analytically such as Khalaf et al. [14].

In this research, influence of rectangular openings existence in composite floor slabs on estimating its effective width was studied experimentally. Rectangular opening shape was chosen rather than another probable opening shapes for the sake of trying to investigate and avoid as possible as could its expected relative undesired effects on structural behavior in general and especially on estimated effective width if it is required to create openings with certain rectangular shape due to some practical or out of hand reasons. To declare the effect of slab opening existence on the effective width, the model with no opening is considered as a reference for the others without for all aspects of analysis and comparison.

INVESTIGATION PROGRAM

Three full-scale models with six different simply supported composite beams (three are intermediate or interior with T-sec. and three are edge or exterior with L-sec.), constant slab rectangularity ($r=0.385$) were tested. One of them is a reference model without slab opening and the others with two symmetric slab openings and constant opening

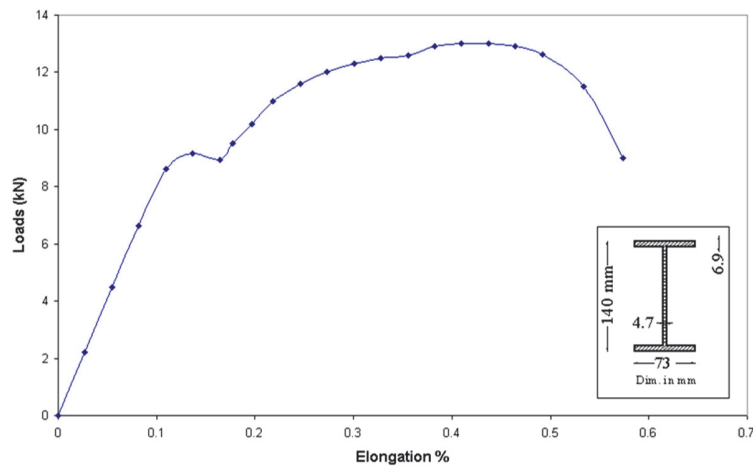


Figure 6: I.P.E 140 Steel section details and tension test results.

Corrugated steel sheet

The geometrical profile dimensions (in mm) of used corrugated sheets are shown in Fig. 7. The geometrical properties are shown in Tab. 3, while Fig. 8 shows the results of the standard tensile test carried out to determine the yield stress and modulus of elasticity. The corrugated sheet was fastened in position to the top of the steel section flange by means of spot welding. This technique was performed specifically to experimental full-scale models of this research to facilitate keeping sheet in position during shear studs welding and enhancing composite slab-beam flange interaction as a basic assumption for reliable structural behavior aspects experimental recordings to estimate composite slab effective width acting as a flange with its supporting steel beams.

Thickness (mm)	Height (mm)	Yield stress (MPa)	Elasticity modulus (MPa)	Area weight /m ² (N)	Volume weight /m ³ (kN)
0.8	30	226.5	196133	57.4	71.98

Table 3: Geometrical properties of used corrugated sheets

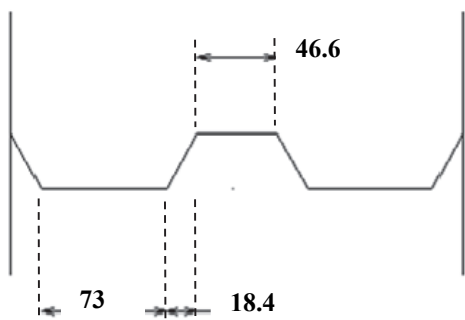


Figure 7: Corrugated steel sheet profile dimensions.

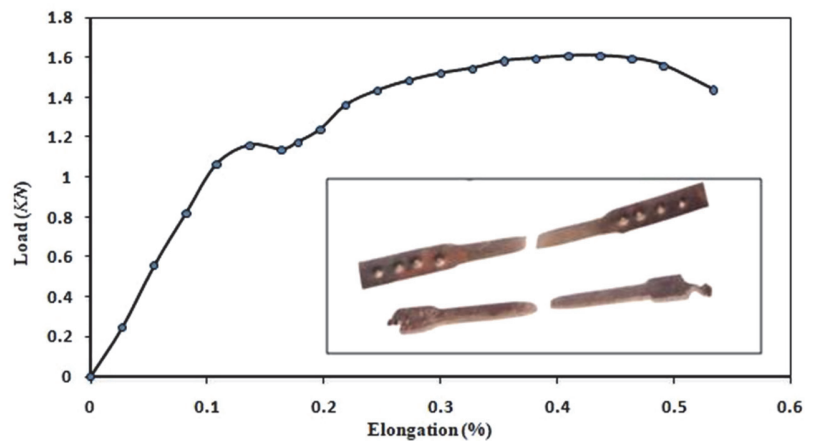


Figure 8: Sheets specimens tensile test results.

Shear transfer devices (Shear studs)

The used shear connectors are screw nails having a diameter of 13mm with a total length of 69mm, head of 18mm diameter and head thickness of 7mm. These dimensions were chosen verifying limits of AISC [16]. The length was chosen so that it passes above the top of the corrugated sheets to prevent shearing of concrete at that level. To achieve full interaction, sufficient number of single shear connectors was used to prevent their probable failure over the main beams

till failure while they were doubled along the edge span quarters as shown in Fig. 9. Also shear connectors spaced by 10 cm is welded along over the secondary beams.



Figure 9: Welded shear studs arrangement along steel beams and sheet ribs; (M3).

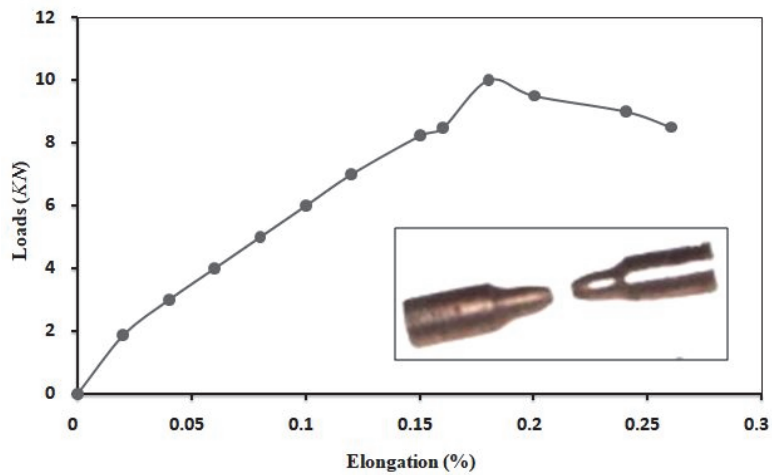


Figure 10: Tensile test results of used shear studs.

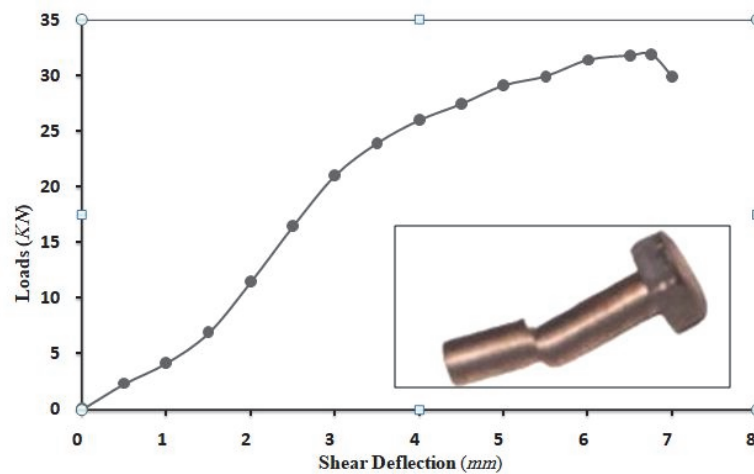


Figure 11: Direct shear test results of used shear studs.



A tensile test was preformed to plot the load-elongation curve as shown in Fig. 10. The modulus of elasticity was found to be 199075MPa, while the yield stress was equal to 243.2MPa. A direct shear test was also performed which resulted in that the maximum shear capacity of the shear connectors equals 242.2MPa. Fig. 11 shows plotting of load-deflection "shear displacement" gained results.

Reinforcing steel bars

The British standard recommended the use of a special steel reinforcing mesh where a concentrated or line loads exerted. So, a top mesh of plain steel bar (6.5 ϕ 6mm/m) in two directions within concrete layer keeping 1.5cm concrete cover was fabricated to resist the negative moments, as shown in Fig.12.



Figure 12: Reinforcing Steel Bars Top Mesh; (M1).

Concrete

The concrete mix is designed to give minimum cube strength of 24.5MPa after 28 days. Tab. (4) shows the used concrete characteristics.

Characteristic	Actual Result		
	M1	M2	M3
Cube Strength after 180 day; f_{cu} (MPa)	32.5	31.8	30.7
Flexural Strength; f_t (MPa)	4.88	4.19	4.07
Modulus of Elasticity *; E_c (MPa)	24923.6	24542.6	24417
Slump Value (cm)	4.5	4.3	4.4
Concrete Volume Weight; γ_c (kg/cm ³)	2377	2370	2390

Table 4: Experimental Models Concrete Characteristics.

*Modulus of elasticity is determined as follows; [17]:

$$E_c = 0.043 \times (\gamma_c)^{1.5} \times (f_c')^{0.5} \text{ where:}$$

E_c : Concrete modulus of elasticity (MPa).

γ_c : Concrete volume weight (kg/m³).

f_c' : Cylinder compressive strength as a function of f_{cu} (MPa); [15].



LOADING SYSTEM ARRANGEMENT

Uniform distributed load

To achieve ultimate benefits of the expensive experimental laboratory fabricated models, all of them were loaded by uniform load (within elastic zone to avoid early bad local effects of concentrated load on models top concrete layers and to achieve; as possible as could; a practical loading manner for early specific ranges of models ultimate capacities). The uniform load was simply achieved by volume weight of uniformly distributed sand layer with total thickness of 10cm which was applied by means of four sequential layers each of 2.5cm thickness to permit recording various structural behavior aspects due to each layer weight application. Each layer represents a uniform load of 4.413MPa with a final total uniform load intensity of approximately 17.652MPa, as shown in Fig. 13.



Figure 13: Final state of sand layers application (uniform distributed load). (a) Uniform load (M1); (b) Uniform load (M2).

Concentrated loads

A steel loading frame (of rigid fabricated hot rolled and built-up section beams system) was designed to perform models testing by means of a hydraulic jack load maximum capacity of 490kN till failure. The jack load was divided to six load points exerting concentrated loads at main supporting steel beams spans thirds; approximately; as shown in Fig. 14.

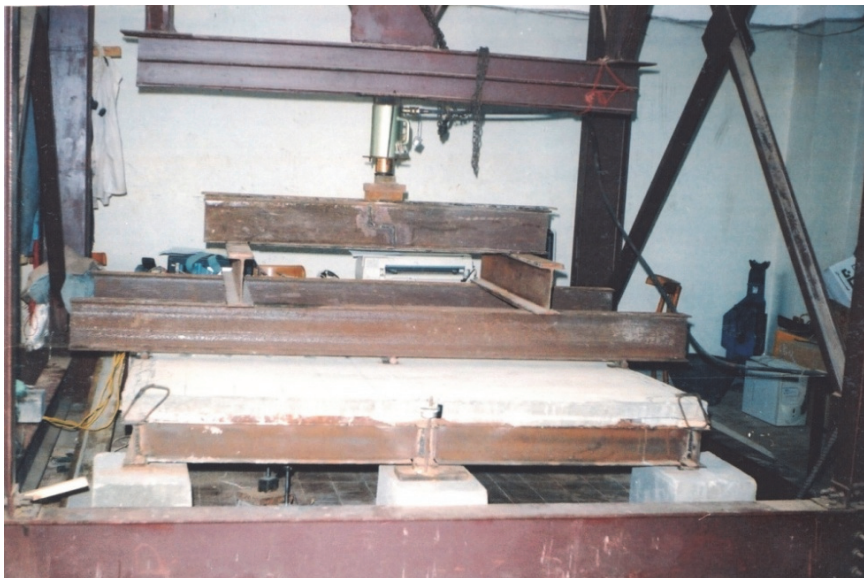


Figure 14: Loading system arrangements (concentrated loads).

MODELS MEASUREMENTS INSTRUMENTATIONS

All models instrumentations seizing laboratory resources as possible as could are globally shown in Fig. 15.

Strain

Two types of strain gauges with length of 20 and 67mm were used to determine the strain in steel and concrete respectively, connected to data-logger, which is instrumented with a printer to record the results as shown in Fig. 16.

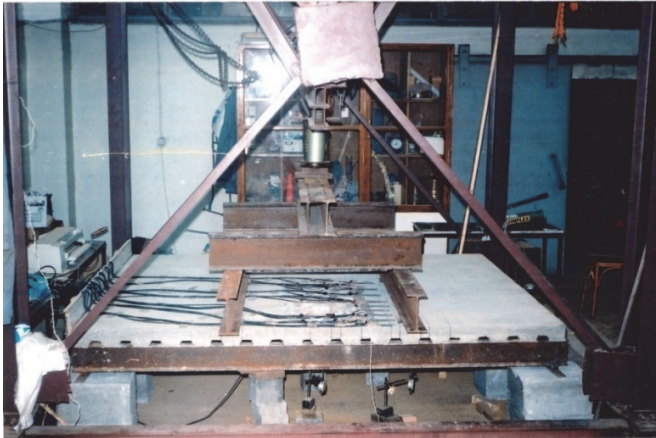


Figure 15: Models measuring instrumentations overview; (M1).

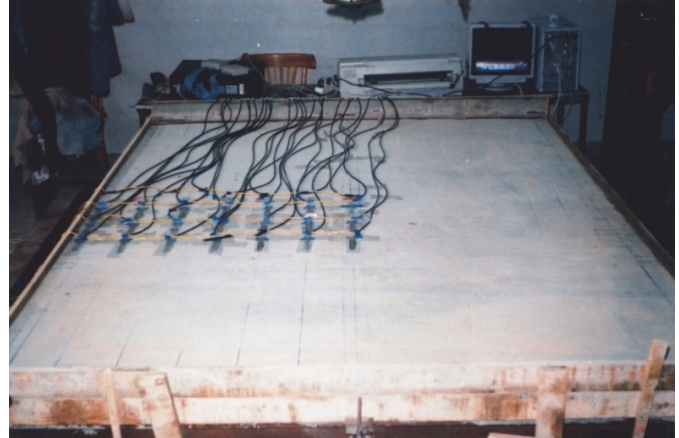


Figure 16: Strain electrical recording system; (M1).

Before casting stage

Electrical sensitive strain gauges (which were embedded in the concrete slab layer) were perfectly attached and fixed to certain reinforced steel bars before pouring concrete to record strain variation for the sake of predicting the effective width of the slab at its mid-span during all loading stages till failure as shown in Fig. 17. For all models, strain readings at bottom flanges mid-span of main supporting steel beams (interior one with T-sec. and two exteriors with L-sec.) were recorded by two attached strain gauges.

After casting stage

The effective width at the slab mid-span and at two sections (solid sections i.e., where steel sheets ribs rested on steel beams) adjacent to previously specified sections (before concrete pouring) were recorded again by means of concrete strain gauges as shown previously in Fig. 16 for model without slab opening which contains nine steel strain gauges and twenty one concrete strain gauges, while models with opening contain nine steel strain gauges and twenty three concrete strain gauge as shown in Figs. 18 and 19.



Figure 17: Embedded steel sheet strain gauges; (M1). (a) Before Concrete Pouring; (b) During Pouring Process.

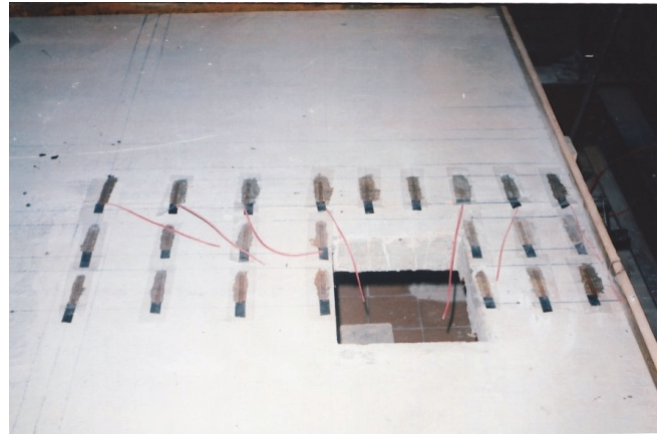


Figure 18: Concrete top layer strain gauges arrangements; (M2).

Figure 19: Concrete top layer strain gauges arrangements; (M3).

More than 7488 readings were recorded by the data-logger during all different loading types and stages for all models (readings were recorded at every loading increment of $w=4.413\text{MPa}$ and $P=1.912\text{kN}$ for uniform and concentrated loads system respectively). The average of three readings for every strain gauge at each loading stage was considered. Fig. 20 simply illustrates the arrangement sketches of strain gauges sensors over all models.

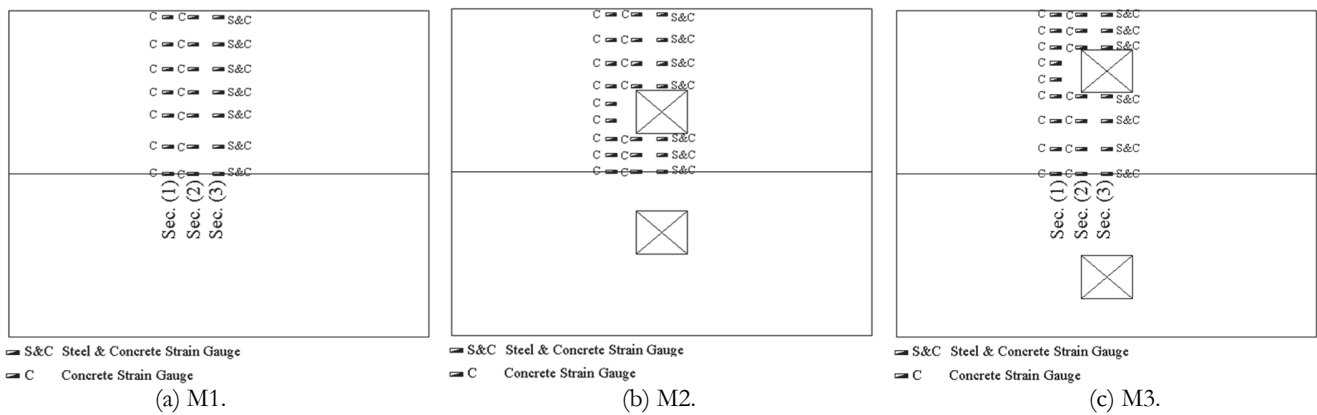


Figure 20: Strain sensors layout sketches over all models.



Figure 21: Dial (5) Position to Record slippage in All Models.



Deflection

Deflection-meters having an accuracy of 0.01mm with a total gauge measuring range of 50mm were used to monitor vertical deflections. Four deflection-meters (two below the positions of concentrated loads and the others at beams mid-spans for interior and exterior beams) were kept in position by means of magnetic bases as shown in Fig. 22. To observe and measure the relative horizontal displacement (slippage) between interior beams (with T-sec.) and its overlaid composite concrete slab, a deflection-meter dial which numbered as (5) was provided as shown in Figs. 21 and 22. More than 390 readings were recorded for all models sequentially at the same loading increments manner as strain recordings.

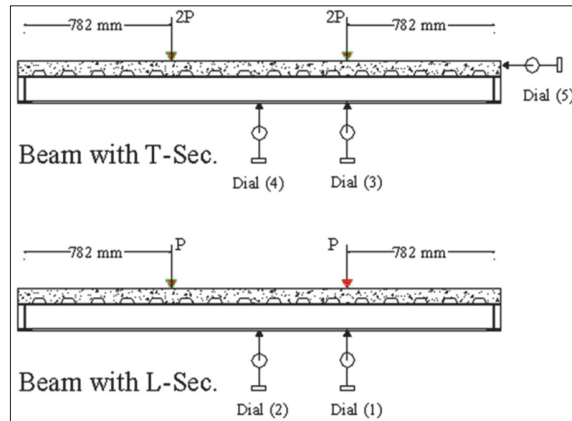


Figure 22: Strain gauges layout sketches over all models.

ANALYSIS AND DISCUSSIONS

The experimental results were recorded, analyzed and discussed guided by tested models mechanical characteristics and structural behavior aspects such as loading type and maximum carrying capacity; cracks pattern, generated strains and deflections at different positions. For the sake of analysis generalization and error minimization, all results were analyzed by means of dimensionless relations. To declare the effect of slab opening existence on its acting effective width with its supporting steel beams, the model with no opening is considered as an analytical reference for other two models with openings for all aspects of analysis and comparison. The openings were in a transverse position of ($y_o=0.64, 0.36$) for models M2, M3 respectively, and with a constant opening longitudinal position of ($x_o=0.5$) as detailed previously in Tab. 1 and Fig. 1.

Deflection due to uniform load

Figs. 23 and 24 show the recorded deflection results assembly for the sake of comparison for all models exterior beams at dials (1 and 2) and interior ones at dials (3 and 4).

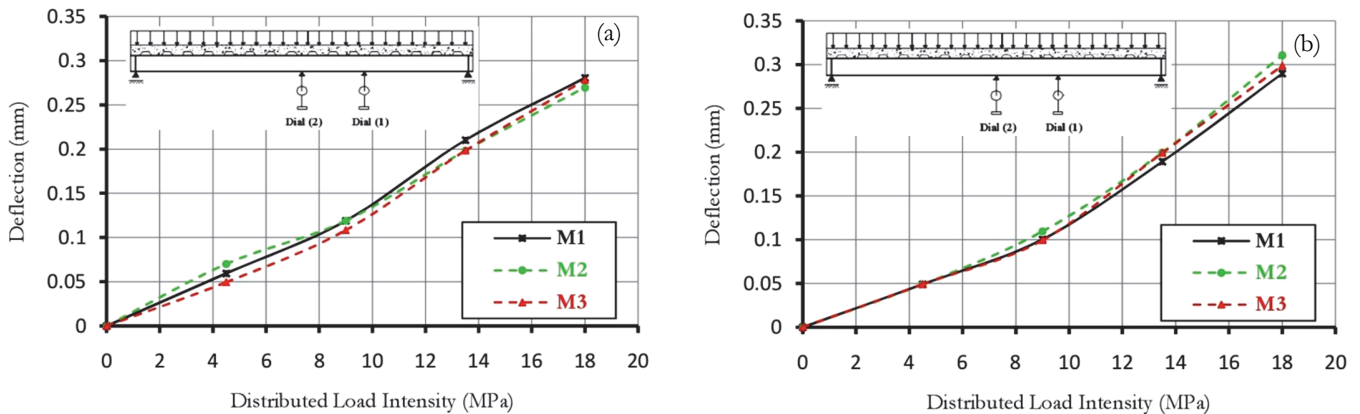


Figure 23: Load intensity vs. deflection for edge or exterior beams. (a) "Beams" ribs parallel, (b) "Girders" ribs perpendicular.

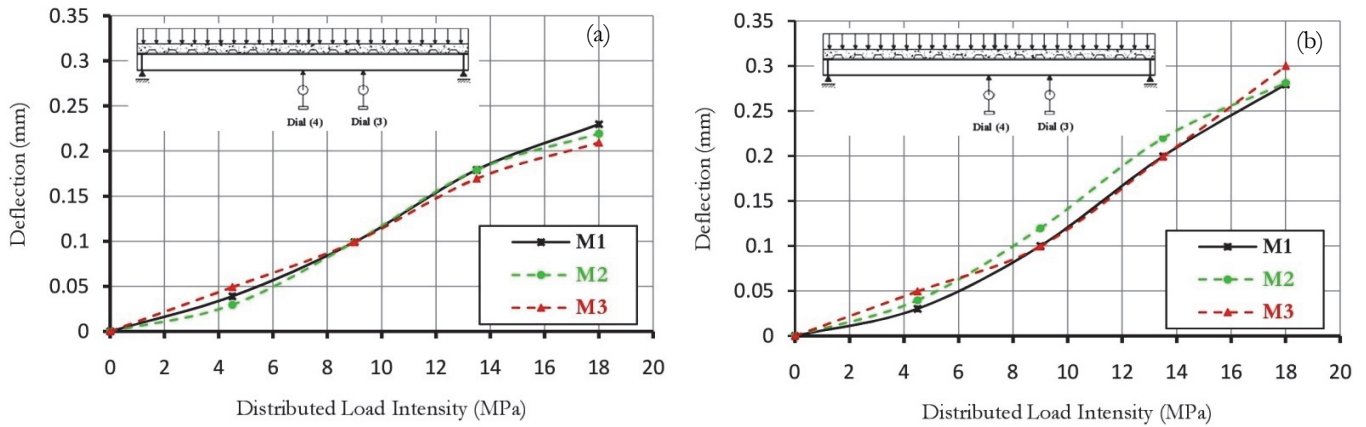


Figure 24: Load intensity vs. deflection for intermediate or interior beams. (a) Dial (3) Readings plotting; (b) Dial (4) Readings plotting.

The pervious figures indicate that there is no noticeable effect of openings existence from deflection point of view on both exterior and interior beams at early elastic stages due to uniform loads.

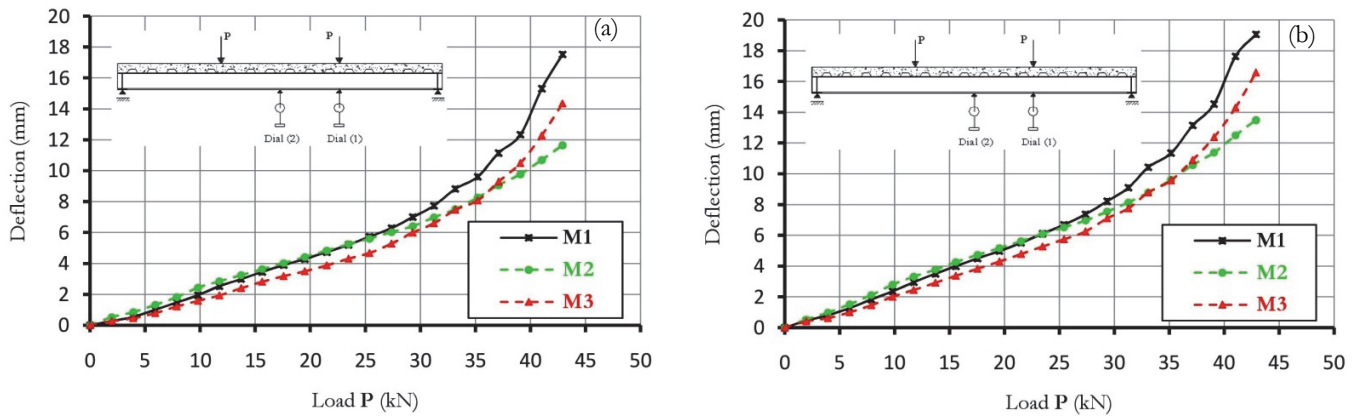


Figure 25: Load intensity vs. deflection for edge or exterior beams. (a) Dial (1) Readings plotting; (b) Dial (2) Readings plotting.

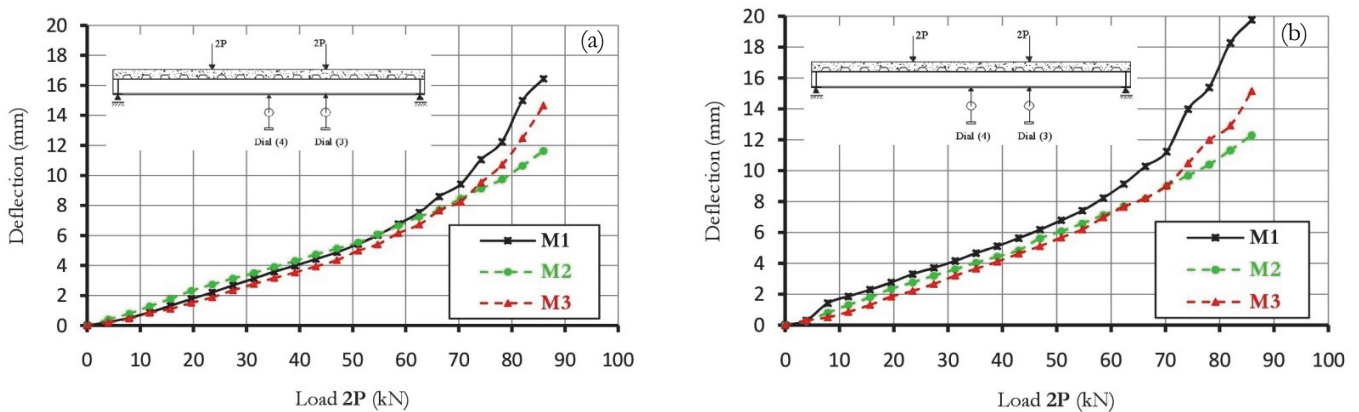


Figure 26: Load intensity vs. deflection for intermediate or interior beams. (a) Dial (3) Readings plotting; (b) Dial (4) Readings plotting.

Deflection due to concentrated loads

Figs. 25 and 26 show the recorded deflection results assembly for the sake of comparison for all models exterior beams at dials (1 and 2) and interior ones at dials (3 and 4).

It can be stated from deflection point of view that a linear behavior is observed up to $78\%P_u$ at both mid-span and beams one third span away from supports of exterior and interior beams for models M1 and M3 and only at mid-span of exterior beam for model M2 while this notice is recorded up to $83\%P_u$ and $72\%P_u$ for exterior and interior beams for model M2 respectively at beams one third span away from supports. Also, this notice is recorded up to $67\%P_u$ for models M1 and



M3 and up to only 61% P_u for model M2 at mid-span of interior beams. Although deflection wasn't the main aim of this research, it can be stated that the opening existence close or near to interior supporting beams (T-section) caused little less undesired effect than for exterior ones (L-section) due to their relatively more rigidities.

The relative horizontal displacement between the interior steel beam and the concrete slab (slippage) initiated at 56%, 39% and 50% P_u for models (M1; M2; M3) respectively as can be stated from Fig. 27. Slippage was limited to only (0.225, 0.125 and 0.32 mm) at failure for models (M1; M2 and M3) respectively, which owing to experimentally achieved full interaction between the steel beams and the composite concrete slabs.

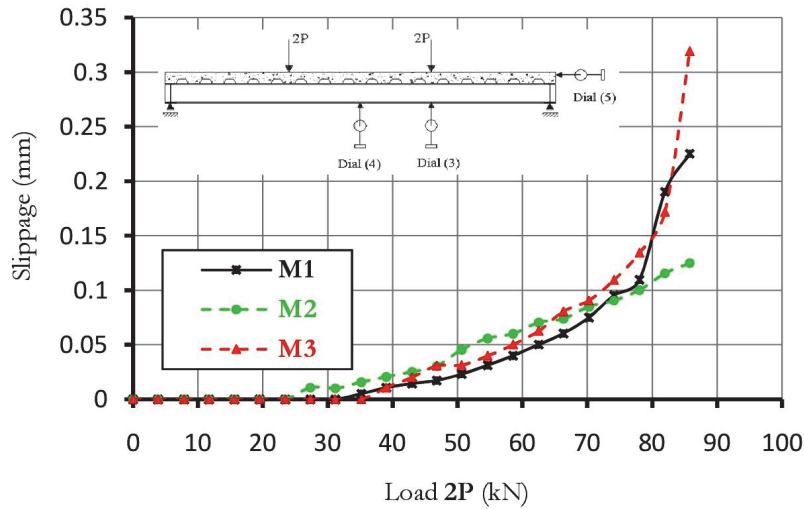


Figure 27: Loading increments vs. slippage for interior beams.

EFFECTIVE WIDTH ESTIMATION

Uniform distributed load

Figures.28 and 29 show the calculated slab effective width as a percentage of structural slab width (ψ) for both exterior and interior beams respectively at three target sections (within span middle third half where sec.3 is located at beam mid-span and sec.1 is located at third of beam span while sec.2 is in between at mid-distance) at maximum applied uniform load of 180kg/m². The strain distribution is more uniform enough to cause no noticeable difference in results at three target sections in model (M1; without openings) due to its composite slab small rectangularity.

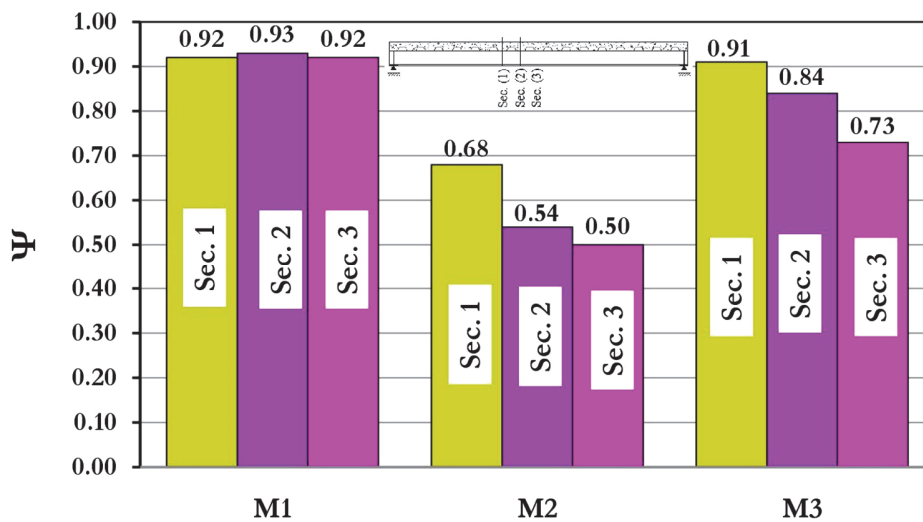


Figure 28: Dial (3) Effective Width of Exterior Beams with (L-section).

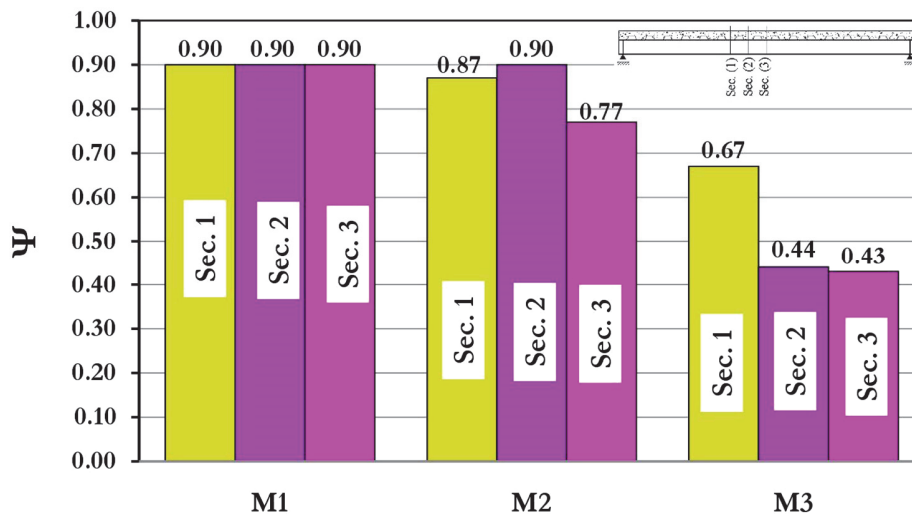


Figure 29: Effective Width of Exterior Beams with (T-section).

It can be deduced that existence of openings in slab more away from exterior beams ($y_o=0.36$) resulted in reduction in the effective width at sec.'s 1, 2 and 3 by only 1.5% , 9.3% and 20% with respect to that without opening while by locating them more closing to it ($y_o=0.64$) decrease the effective width by 26.5% , 43.1% and 45.7% respectively. It is also observed that the effective width at section sec.1 has approximately the same vales for M1 and M3.

On the other hand, existence of openings in slab more away from interior beams ($y_o=0.64$) resulted in reduction in the effective width at sec.'s 1, 2 and 3 by only 3.3%, 0% and 14.5% with respect to that without opening while by locating them more closing to it ($y_o=0.36$) decrease the effective width by 25.4%, 50.8% and 52.3% respectively. It is obvious that the effective width at section sec.2 has exactly the same vales for M1 and M2.

Finally, locating the openings more away from supporting steel beams as possible as could makes their existence undesired effects on estimated effective width decreased as structurally preferred.

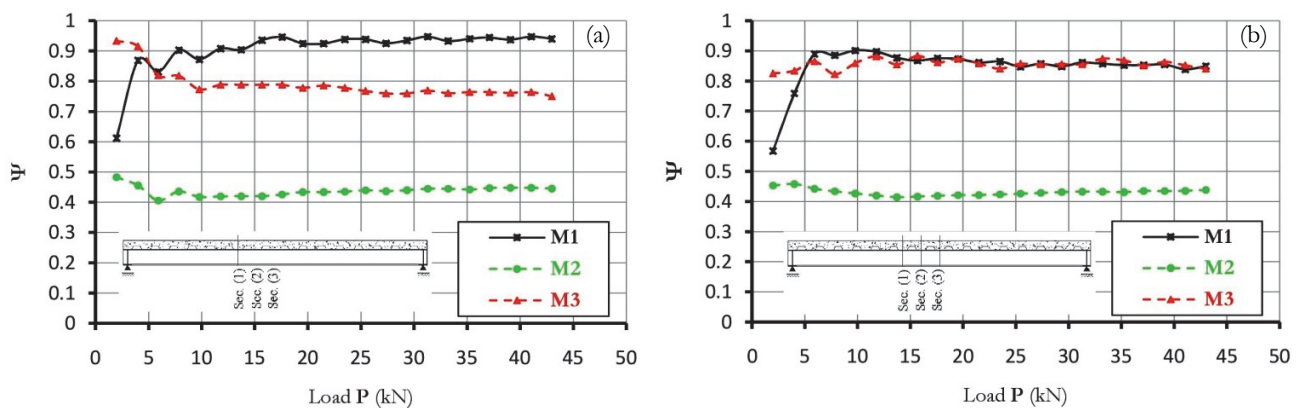


Figure 30: Influence of loading increments vs. effective width for exterior beams. (a) Sec.2; (b) Sec.3.

Concentrated loads

Unfortunately, recorded results of estimated effective width at sec.1 are suppressed from analysis as a result of its location duo to their interruptions where high stress concentrations existed; as initially expected; at regions in vicinity to concentrated loads points of applications.

Fig. 30 represents the normalized effective width (ψ) at sec.'s 2 and 3 for exterior supporting steel beams due to different loading levels till failure. Except some interrupted results at start, there is no noticeable difference in effective width estimated at mid-span (sec.3) for models M1 and M3 which may be interpreted by locating openings more away enough from beams axes. In the other hand, the effective width at Sec. 2 in model (M3) decreased by about 20% in average compared to that for model (M1) which may be due to its closer location to stress concentration region near openings corners. For model (M2) where openings are located closer to exterior beams axes, the effective width estimated at both



sections 2 and 3 was decreased by 50% in average compared to that of reference model without opening (M1). This great reduction is due to openings which were located within structural areas carried by exterior beams which relatively reduced constantly their structural capacities during loading stages.

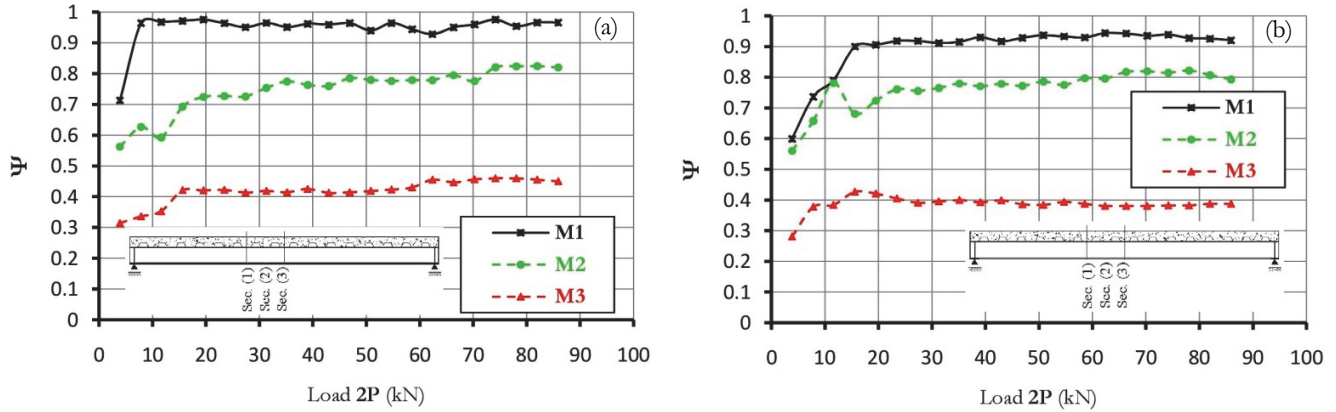


Figure 31: Influence of loading increments vs. effective width for interior beams. (a) Sec.2; (b) Sec.3.

Fig. 31 represents the normalized effective width (ψ) at Sec.'s 2 and 3 for interior beams till failure. Regardless observed fluctuation of recorded results at early loading stages; the slab estimated effective width at sec.'s 2 and 3 for model (M2) decreased by 25% and 20% in average at 39% and 79%Pu compared to that for reference model without opening respectively, while it decreased to be only 15.5% before failure (123%Pu). These statements are unlike those recorded for exterior beams. As previously deduced for model (M2) concerned with exterior beams; Fig. 30, the same conclusions can be stated where openings are far away enough from interior beams in model (M3).

The fluctuation of estimated slab effective width values at sections 2 and 3 for model (M1, M2, M3) were limited to 6% and 3% and 8% in average during all loading stages for exterior beams while these ratios were only 4.5%, 2.5% and 3.5% in average for model (M1, M2, and M3) respectively for interior beams.

For the sake of constituting an overview for effect of loading types and openings locations on composite slab acting as effective width (b_e) of supporting steel beam for design purposes, a factor (ψ_d); [minimum value of (b_e) within middle third of beam span compared to composite slab structural loading area width (b^*) carried by supporting steel beam] was introduced.

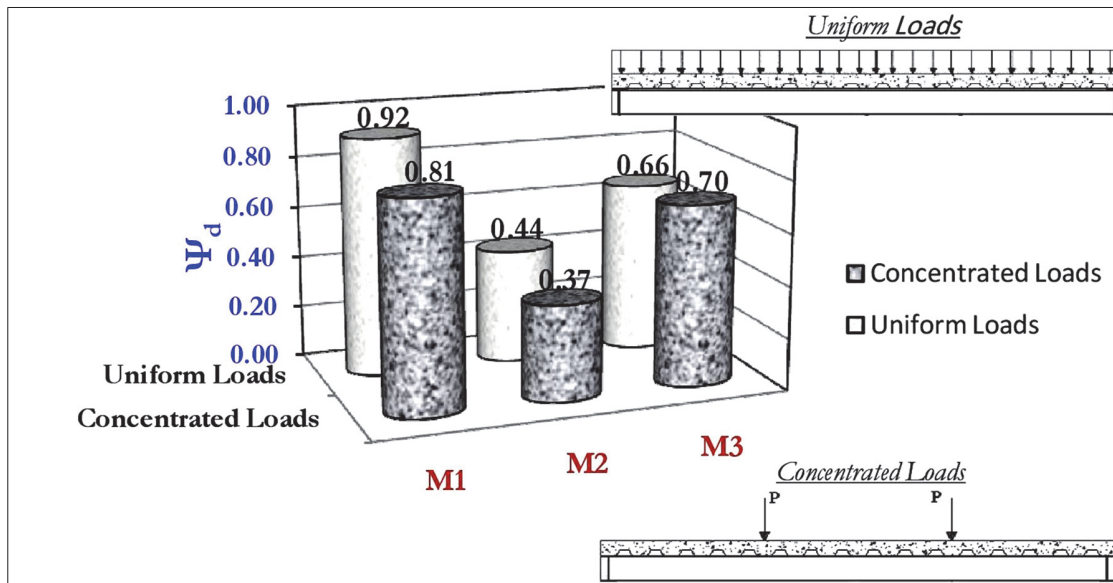


Figure 32: Influence of loading type and opening location on effective width for exterior beams with L-sec; (ψ_d).

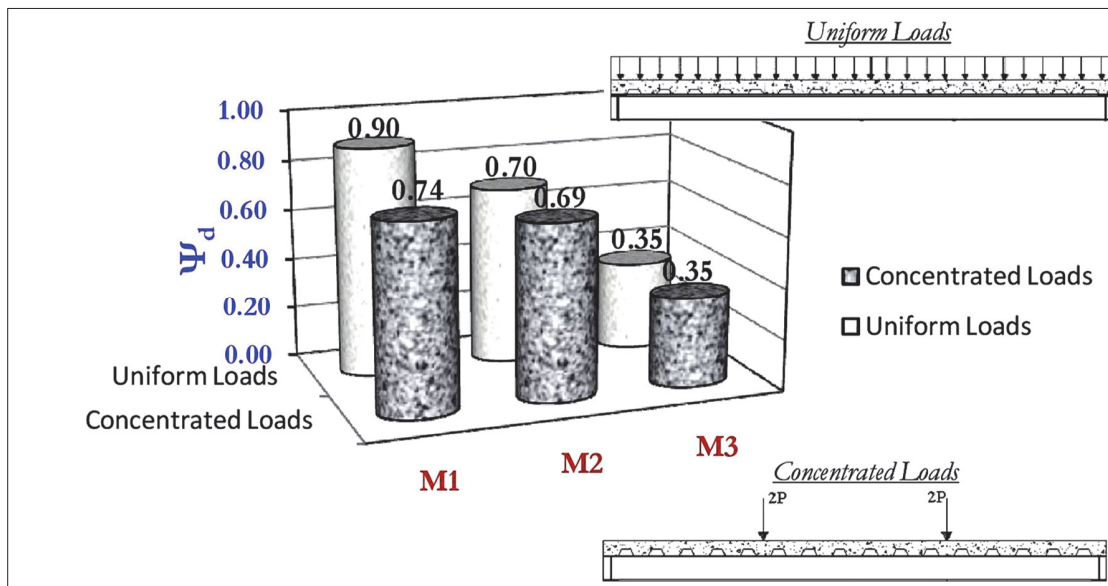


Figure 33: Influence of loading type and opening location on effective width for interior beams with T-sec; (ψ_d).

As can be deduced from Fig. 32 for exterior beams within range of uniform loading exerted intensity resultant, (ψ_d) was decreased by 12% and 15.9% for (M1, M2) respectively when loaded by concentrated loading type compared to those loaded by a uniform load, while in contrary, this ratio was only 6.7% when loaded by uniform load compared to concentrated loading case for (M3). Locating openings closer to the beams longitudinal axes ($y_o = 0.64$) reduced (ψ_d) to be 47.1% and 33.3% for concentrated and uniform loading types respectively compared with case of relatively away locations from the supporting steel beams ($y_o = 0.36$).

Fig. 33 declares that (ψ_d) for interior beams, was decreased by 17.8% and 1.4% for (M1, M2) respectively when loaded by concentrated loading type compared to those loaded by a uniform load, while on the other hand, no significant effect was recorded in (ψ_d) due to model (M3) loading by both loading types within range of uniform loading exerted intensity resultant. Locating openings closer to interior beams longitudinal axes ($y_o = 0.36$) reduced (ψ_d) to be 49.3% and 50% for concentrated and uniform loading types respectively compared with case of relatively away locations from the supporting steel beams ($y_o = 0.64$) which indicates serious influence of (y_o) [openings transverse positions] on (ψ_d).

Finally, previous analysis declares how much composite slab openings existence had a seriously undesired effect on effective width of slab acting as flange with supporting steel beams especially where openings are located near to beams longitudinal axes.

CONCRETE CRACKS PATTERNS AND FAILURE MODES

The maximum laboratory exerted uniform load intensity of only 1.765kN/m² was not enough to force experimental constructing composite slab models to reach failure or even yielding state so, the failure modes and cracks patterns are only analyzed due to laboratory specially fabricated concentrated loading system as detailed before.

Fig. 34 shows a concrete cracks pattern for reference model (M1). Firstly, a separation between steel sheet and overlaid reinforced concrete slab was observed at its both edges perpendicular to steel corrugations direction after which concrete cracks was initiated at its bottom interface with steel sheet within in between distances of concentrated loads and supports; (shear cracks). Also, this failure mode sequential description can be typically stated for other two models with openings M2 and M3 as shown in Fig. 35. These cracks went to be wider more and more and inclinable propagated towards surface top while other cracks initiated within two concentrated loads in between distance slightly before failure where cracks appeared along overall concrete slab top surface especially within spans middle thirds of both exterior and interior supporting steel beams accompanied with concrete crushing. Also, concrete cracks (longitudinal separation cracks) appeared at failure along steel sheet edges above secondary steel beams.



Figure 34: Failure mode and cracks pattern for reference model M1. (a) Perspective view; (b) Profile.

Generally, great similarity in failure modes and concrete crack patterns of reference model (M1) was detected for models with openings (M2 and M3) except that initiation and propagation of concrete cracks occurred within the two applied concentrated loads in between distance before regions within composite slab span edge thirds; as shown in Fig. 35; which was owing to openings existence and; consequently; their effect of generating stress concentration areas neighboring openings boundaries within these regions as structurally and logically expected. Fig. 35 declares typical failure mode views for models with openings; M2 and M3.

In addition, Fig. 36 shows a composite slab bottom view to declare typical excessive deformation and yielding state of steel beams and sheets at failure.

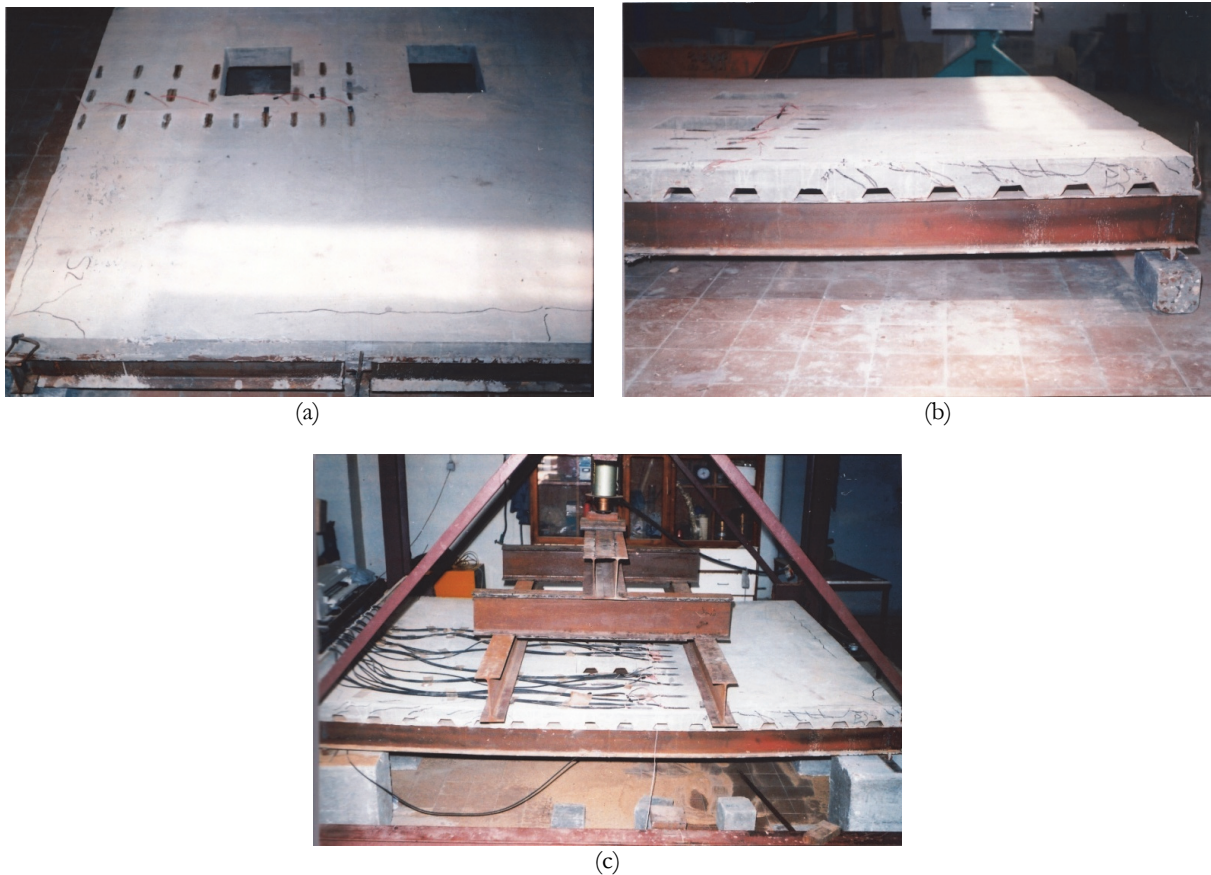


Figure 35: Typical failure mode and cracks pattern for models with openings; M3. (a) Clean plan view; (b) Profile view; (c) Perspective under loading view.



Figure 36: Typical steel beams and steel sheets yielding state for all models.

CONCLUSIONS AND RECOMMENDATIONS

Based on current achieved experimental laboratory work, many important conclusions which may be useful for designers concerning with openings existence in composite slabs and recommendations for future work are stated here in brief as follows:

- 1- Locate the opening; if any; out of boundaries (width) of structurally carried slab zone by the supporting steel beams (or as far away as possible from the beam longitudinal axis).
- 2- If it is required to be closer to supporting beam longitudinal axis, locate the opening keeping its corners as far away as possible from the middle third of the beam span. So, round opening corners are seriously recommended especially in this case and generally at all to avoid existence of stresses concentrations generation zones.
- 3- Interior supporting steel beams are slightly more affected due to opening existence within or close to their structurally carried composite slab regions than exterior ones.
- 4- Concentrated loading type reduced effective width of composite slab without openings acting as a flange with its supporting steel beams to be about 88% and 82% compared to that loaded by equivalent uniform load intensity for exterior and interior beams respectively. In other words, concentrated loads manner reduced carried composite slab effective width to be 85% in average of that recorded for equivalent distributed loads.
- 5- Opening existence in a composite slab within its span middle third cross to supporting steel beams; in spite of its being out of its structural carried width by beams ($y_o=0.64$); reduces its effective width as a flange with its supporting steel beams to be maximum of about 68% and 70% in average compared to that without opening for exterior and interior beams respectively regardless to loading type.
- 6- Opening existence in a composite slab within its span middle third cross to supporting steel beams and within its structural carried width by beams ($y_o=0.36$) reduces its effective width as a flange with its supporting steel beams to be maximum of about 40% and 35% in average compared to that without opening for exterior and interior beams respectively regardless to loading type.
- 7- It can be stated that more than 100% of slab effective width is preserved for interior supporting beams if the openings are away enough from carried composite slabs structural carried zones while only 70% was preserved for exterior ones.
- 8- It is recommended to numerically extend this research to study more and more structural parameters effects on estimated effective composite slab acting as a flange with supporting steel beams which will be done in a next research paper.

REFERENCES

- [1] Fraser, D.J. (1971). The effective widths of simply-supported T and L beams for the calculation of deflections, The National Library of Australia, Kensington, N.S.W., School of Civil Engineering, University of New South Wales, 1971, UNICIV Report ; No. R-66, Bib ID: 938997, ISBN: 085841 006 0. Available at: <https://catalogue.nla.gov.au/Record/938997>



- [2] Adekola, A. O., Moffatt, KR., Lim, PTK (1974). On the influence curves for effective width in non-prismatic composite beams, *Proceedings of the Institution of Civil Engineers, London, England* 57(3), pp. 553-557, DOI: 10.1680/iicep.1974.4034
- [3] Elkelish, S., Robinson, H. (1986). Effective widths of composite beams with ribbed metal deck, *Canadian Journal of Civil Engineering* 13(5), pp. 575-582, DOI: 10.1139/l86-084
- [4] Chen, S.S., Aref, A.J., Ahn, I.-S., Chiewanichakorn, M. J., Carpenter, Nottis, A. A. and Kalpakidis, I. (2005). Effective slab width for composite steel bridge members, Dept. of Civil, Structural and Environmental Engineering, State University of New York at Buffalo, Buffalo, NY, DOI: 10.17226/13853.
- [5] Bortsch, R. (1921). Die Mitwirkende Plattenbreite (The Plate Width Contributors). *Der Bauingenieur (The Civil Engineer)*, 23, pp. 662 - 667 (in German).
- [6] Chapman, J. C. and Teraskiewicz, J. S. (1968). Research on composite construction, Imperial college Proceedings of the conference on steel bridges, Institution of Civil Engineers, Great George Street, London SW1, British Constructional Steelwork, TG416.C66, London, England, 24-26 June, 257 PP.
- [7] Amadio, C. and Fragiaco, M. (2002). Effective width evaluation for steel-concrete composite beams, *Journal of construction steel research*, 58, pp. 373-388, DOI: 10.1016/S0143-974X (01)00058-X.
- [8] Amadio C, Briganti D. (2004). Experimental evaluation of effective width in steel-concrete composite beams, *Journal of constructional steel research*, 60, pp.199-220, DOI: 10.1016/j.jcsr.2003.08.007 .
- [9] Mackey, S. W., Franklin K. C., (1961). The Effective Width of a Composite Tee-Beam Flange, *The Institution of Structural Engineers, International HQ*, 47-58 Bastwick Street, London, EC1V 3PS, 277. Available at: [https://www.istructe.org/journal/volumes/volume-39-\(published-in-1961\)/issue-9/the-effective-width-of-a-composite-tee-beam-flange/#.YipxSCzme30.link](https://www.istructe.org/journal/volumes/volume-39-(published-in-1961)/issue-9/the-effective-width-of-a-composite-tee-beam-flange/#.YipxSCzme30.link)
- [10] Lee, J.A.N., (1962). Effective Widths of Tee-Beams, *The Institution of Structural Engineers, International HQ*, 47-58 Bastwick Street, London, EC1V 3PS, 21. Available at: [https://www.istructe.org/journal/volumes/volume-40-\(published-in-1962\)/issue-1/effective-widths-of-tee-beams/#.YiqBtzUoFak.link](https://www.istructe.org/journal/volumes/volume-40-(published-in-1962)/issue-1/effective-widths-of-tee-beams/#.YiqBtzUoFak.link)
- [11] Brendel, G. F., (1964). Strength of the compression slab of T-beams subject to simple bending, *Journal of American Concrete Institute ACI, Journal Proceedings*, 61, pp. 57-76.
- [12] Sabnis, G.M., (1979). *Handbook of Composite Construction Engineering*, Van Nostrand Reinhold Publishing Company, New York, 380. Available at: <https://www.worldcat.org/title/handbook-of-composite-construction-engineering/oclc/4004913>.
- [13] Amadio, C., Fedrigo, C., Fragiaco, M., (2004). Experimental evaluation of effective width in steel concrete composite beams, *Journal of Constructional Steel Research*, 60, pp. 199-220, DOI: 10.1016/j.jcsr.2003.08.007.
- [14] Khalaf, M., El-Shihy, A., El-Kasaby, E., and Youssef, A., (2014). Numerical estimation and analysis of effective width of composite beams with ribbed slab, *International Journal of Application or Innovation in Engineering & Management (IJAIEM)*, 3(8), pp. 1-15. Available at: <https://www.ijaiem.org/issue1.php?vol=Volume3Issue8>.
- [15] HBRC, Housing and Building National Research Center; (2001). *Egyptian Code of Practice for Reinforced Concrete Structures Design & Construction, ECP 203-2001, 2nd upgrading version, Appendix "3"; Laboratory Testing Guide for Concrete Construction Materials*, Permanent Technical Committee, Cairo, Egypt.
- [16] American Institute of Steel Construction AISC, (1999). *Load and Resistance Factor Design Specification for Structural Steel Buildings*, AISC, INC., One East Wacker Drive, Suite 3100, Chicago, Illinois 60601-2001.
- [17] Wang, C. K., Salmon, C.G., (1985). *Reinforced Concrete Design*, Harper & Row Publishers Inc., 10 East 53d Street, New York, NY 10022, 4th Edition, TA683.2.W3-1985, 940.

NOMENCLATURE

- b^* : Composite slab structural supported area width carried by its supporting steel beam.
 b_e : Composite slab effective width.
 b_{emin} : Minimum estimated effective width within supporting steel beam spanmiddle third.
 d_x : Opening centroid distance away from main supporting steel beam left support; (Fig. 5).
 d_y : Opening centroid distance away from main supporting steel beam longitudinal axis; (Fig. 5).
 h : Steel beam cross section height.
 h_t : Overall section depth.
 L_1 : Main supporting steel beams spans; (Fig. 5).



- L_2 and L_3 : Floor panels and edge secondary beams spans; (Fig. 5).
 L_{o1} : Opening length; (Fig. 5).
 L_{o2} : Opening width; (Fig. 5).
 P_u : Models design ultimate load capacity.
 r_o : Opening aspect ratio or opening rectangularity; ($r = L_{o1}/L_{o2}$); (Fig. 5).
 r_1 : Opening longitudinal orientation position; ($r_1 = L_{o1}/L_1$); (Fig. 5).
 r_2 : Opening transverse orientation position; ($r_2 = L_{o2}/L_2$ or $r_2 = L_{o2}/L_3$); (Fig. 5).
 x_o : Opening normalized longitudinal position; ($x_o = d_x/L_1$); (Fig. 5).
 y_o : Opening normalized transverse position; ($y_o = d_y/L_2$); (Fig. 5).
 z : Normalized steel beam span factor; (considered section distance away from supports compared to beam span).
 Ψ : Normalized composite slab effective width factor; ($= b_e/b^*$).
 Ψ_d : Normalized composite slab design effective width factor, ($= b_{e,min.}/b^*$).